

# Necking of a hyperelastic solid cylinder under axial stretching: evaluation of the infinite-length approximation

Mi Wang<sup>a</sup>, Yibin Fu<sup>b,\*</sup>

<sup>a</sup>*Department of Mechanics, Tianjin University, Tianjin 300072, China*

<sup>b</sup>*School of Computing and Mathematics, Keele University, Staffordshire ST5 5BG, UK*

---

## Abstract

A weakly nonlinear analysis is conducted for localized necking of a hyperelastic solid cylinder under axial stretching based on the exact theory of nonlinear elasticity. The amplitude equation derived is shown to be consistent with the one-dimensional model recently proposed by Audoly and Hutchinson (J. Mech. Phys. Solids **97**, 2016, 68-91). It is shown that results based on the infinite-length approximation are sufficiently accurate even for cylinders with very moderate length/diameter ratios. In contrast, a weakly nonlinear analysis based on the finite length is only valid for very stubby cylinders and for axial force much closer to its bifurcation value than anticipated.

*Keywords:* Localized necking, hyperelasticity, nonlinear analysis, bifurcation, stability.

---

## 1. Introduction

Necking is a phenomenon commonly observed in the tension test of ductile materials. It has also been observed in semi-crystalline polymers (Carothers & Hill, 1932), and glassy polymers (Whitney & Andrews, 1967; Crissman & Zapas, 1974; Zapas & Crissman, 1974; Ward & Sweeney, 1982). Numerical simulations of necking in plastic materials have been conducted by Chen (1971), Needleman (1972), Norris et al. (1978), Burke & Nix (1979), and Silling (1988). Analyses based on one-dimensional (1D) models have been conducted by Barenblatt (1964), Antman (1972), Antman (1973), Ericksen (1975), Triantafyllidis & Aifantis (1986), Owen (1987), Coleman (1983), Coleman & Newman (1988), Dai & Bi (2006), but such 1D models are usually not self-consistent in the sense that not all relevant terms are kept at every order of the approximate solution. Notable exceptions are those derived from the three-dimensional theory by Dai et al. (2008), Dai & Peng (2012), and more recently Audoly & Hutchinson (2016). Necking has also been conducted based on the nonlinear elasticity theory by treating necking as a periodic mode admitted by the incremental equations;

---

\*Corresponding author at: School of Computing and Mathematics, Keele University, Staffordshire ST5 5BG, UK

*Email address:* [y.fu@keele.ac.uk](mailto:y.fu@keele.ac.uk) (Yibin Fu)

see Wesolowski (1962), Hill & Hutchinson (1975), Antman & Carbone (1977), Scherzinger & Triantafyllidis (1998), Triantafyllidis et al. (2007). Constitutive behaviour that gives rise to necking has been investigated by Leonov (2002). Commonly used hyperelastic material models such as neo-Hookean, Mooney-Rivlin, Ogden, and Gent strain-energy functions do not allow necking under entirely mechanical loading, but subject to additional effects such as electric actuation or surface tension, necking becomes commonplace; see Fu et al. (2018) and Fu et al. (2020).

Except for the analysis by Mielke (1991) and Fu (2001), it has been customary in the literature to treat localized necking as a bifurcation initiated from a *periodic* mode satisfying special types of end conditions. The same practice prevailed in the studies of localized bulging of inflated rubber tubes for many years. However, recent numerical simulations and experimental studies carried out by Wang et al. (2019) have shown that localized bulging in the latter problem is fairly insensitive to end conditions when the length/diameter ratio exceeds a fairly moderate value; it is appropriate to treat localization as a bifurcation problem with zero wave number and view end effects as imperfections, as in the approach of center-manifold reduction. Our current study is motivated by the study of Audoly & Hutchinson (2016) which provides us with a convenient platform to assess the effect of finite length on localized necking. It may be viewed as an extension of the study by Fu (2001) from the plane strain case to the 3D case with the use of the perturbation approach. We remark that although the perturbation approach is less rigorous than the center-manifold reduction, the two approaches have almost always yielded the same amplitude equations/normal forms.

The rest of this paper is divided into five sections as follows. After formulating the necking problem in the next section, we apply in Section 3 the perturbation approach to derive the amplitude equation that governs the shape and character of the localized solutions. In Section 4 we present a slightly simplified version of the analysis given by Audoly & Hutchinson (2016) and show that this approach yields the same amplitude equation as the perturbation approach. In Section 5 we discuss the question “how long should the cylinder be, when describing necking, for it to be treated effectively as a cylinder of infinite length”. The paper is then concluded with a summary that highlights our main findings.

## 2. Problem formulation

We first summarize the governing equations for a general homogeneous elastic body composed of a non-heat-conducting incompressible elastic material. Such a material is assumed to possess an initial unstressed configuration  $\mathcal{B}_0$ . A finite static deformation (not necessarily homogeneous) is imposed upon  $\mathcal{B}_0$  to produce an equilibrium configuration denoted by  $B_e$ . To determine whether this finitely deformed configuration is unique or not, we superimpose

on  $\mathcal{B}_e$  a small amplitude perturbation that brings the material body to the current configuration denoted by  $\mathcal{B}_t$ . Relative to a common coordinate system the position vectors of a representative material particle in the three configurations are denoted by  $\mathbf{X}$ ,  $\mathbf{x}$  and  $\tilde{\mathbf{x}}$ , respectively, and we write

$$\tilde{\mathbf{x}} = \mathbf{x} + \mathbf{u}(\mathbf{x}), \quad (2.1)$$

where  $\mathbf{u}$ , as a vector function of  $\mathbf{x}$ , denotes the incremental displacement field from  $\mathcal{B}_e$  to  $\mathcal{B}_t$ . The  $\mathbf{x}$  itself is a function of  $\mathbf{X}$ . We define deformation gradient tensors  $\bar{F}$  and  $\tilde{F}$  by

$$d\mathbf{x} = \bar{F}d\mathbf{X}, \quad d\tilde{\mathbf{x}} = \tilde{F}d\mathbf{X}. \quad (2.2)$$

With the use of (2.1), we also have

$$d\tilde{\mathbf{x}} = (I + \text{grad } \mathbf{u})d\mathbf{x} = (I + \eta)\bar{F}d\mathbf{X},$$

where  $\eta = \text{grad } \mathbf{u}$  denotes the gradient of  $\mathbf{u}$  with respect to  $\mathbf{x}$ . It then follows that

$$\tilde{F} = (I + \eta)\bar{F}. \quad (2.3)$$

We assume that the constitutive behaviour of the material is described by the strain-energy function  $W(F)$  measured per unit volume in the reference configuration such that the nominal stress  $S$  is given by

$$S = \frac{\partial W}{\partial F} - pF^{-1}, \quad (2.4)$$

where  $p$  is the Lagrangian multiplier associated with the constraint of incompressibility  $\det F = 1$  and will subsequently be referred to as the constraint pressure. Specialized to the deformation  $\mathcal{B}_0 \rightarrow \mathcal{B}_e$ , the constitutive equation (2.4) defines the nominal stress  $\bar{S}$  and the constraint pressure  $\bar{p}$ . The equilibrium equations for the configurations  $\mathcal{B}_e$  and  $\mathcal{B}_t$  are given by

$$\text{Div } \bar{S} = \mathbf{0}, \quad \text{Div } \tilde{S} = \mathbf{0}, \quad (2.5)$$

respectively, where Div is the divergence operator with respect to  $\mathbf{X}$  and  $\tilde{S}$  denotes the nominal stress associated with the deformation  $\mathcal{B}_0 \rightarrow \mathcal{B}_t$ . For the purpose of bifurcation analysis, it is convenient to define an incremental stress tensor  $\chi$  through

$$\chi^T = \bar{J}^{-1}\bar{F}(\tilde{S} - \bar{S}), \quad (2.6)$$

where the superscript T stands for transpose, and  $\bar{J}$  denotes the determinant of  $\bar{F}$  (which is unity in the current case but is kept in the formula to maintain the generality of the formula). With the use of (2.5) and the identity  $\text{div } \bar{J}^{-1}\bar{F} = \mathbf{0}$  where div denotes the divergence with respect to  $\mathbf{x}$ , we obtain

$$\text{div } \chi^T = \mathbf{0}. \quad (2.7)$$

By straightforward Taylor expansion around the finite deformation  $(\bar{F}, \bar{p})$ , equation (2.6) together with (2.4) yields (Fu & Rogerson, 1994)

$$\chi_{ij} = \mathcal{A}_{jilk}\eta_{kl} + (\bar{p} + p^*)\xi_{ji} - p^*\delta_{ji} + \frac{1}{2}\mathcal{A}_{jilknm}^2\eta_{kl}\eta_{mn} + \dots, \quad (2.8)$$

where the tensor components  $\xi_{ji}$  are defined by

$$\xi_{ji} = (I - \bar{F}\bar{F}^{-1})_{ji} = \eta_{ji} - \eta_{jm}\eta_{mi} + \dots, \quad (2.9)$$

$p^*$  is the incremental constraint pressure associated with the deformation  $\mathcal{B}_e \rightarrow \mathcal{B}_t$ , and  $\mathcal{A}_{jilk}$  and  $\mathcal{A}_{jilknm}^2$  are the 1st- and 2nd-order instantaneous elastic moduli (Chadwick & Ogden, 1971). The  $\mathcal{A}_{jilk}$  are given by

$$\mathcal{A}_{jilk} = \bar{J}^{-1}\bar{F}_{jA}\bar{F}_{lB} \left. \frac{\partial^2 W}{\partial F_{iA}\partial F_{kB}} \right|_{\mathbf{F}=\bar{\mathbf{F}}}, \quad (2.10)$$

and  $\mathcal{A}_{jilknm}^2$  are defined in a similar manner. Their expressions in terms of the principal stretches can be found in Ogden (1984) or Fu & Ogden (1999). Note that the above expressions are valid for any coordinate system, and the tensor  $\xi$  enjoys the property that  $\text{div } \xi = \mathbf{0}$ .

When (2.8) is substituted into (2.7), the resulting expression can be simplified by making use of the fact that  $\text{div } \xi = 0$ . More precisely, we shall replace (2.7) by

$$\mathbf{l} \equiv \text{div } \chi^T - (\bar{p} + p^*) \text{div } \xi = \mathbf{0} \quad (2.11)$$

in the subsequent derivations.

On any part of the material boundary that is traction-free, we have  $\tilde{S}^T \mathbf{N} = \mathbf{0}$ ,  $\bar{S}^T \mathbf{N} = \mathbf{0}$ , and hence  $\chi \mathbf{n} = \mathbf{0}$ , where  $\mathbf{N}$  and  $\mathbf{n}$  denote the unit normals to the boundary in  $\mathcal{B}_0$  and  $\mathcal{B}_e$ , respectively.

We now specialize the above governing equations to the case when the material body is a solid circular cylinder which has radius  $A$  in  $\mathcal{B}_0$ . The finite deformation from  $\mathcal{B}_0$  to  $\mathcal{B}_e$  corresponds to a uni-axial tension in the axial direction so that  $\bar{F}$  takes the form

$$\bar{F} = \frac{1}{\sqrt{\lambda}} \mathbf{e}_r \otimes \mathbf{e}_r + \frac{1}{\sqrt{\lambda}} \mathbf{e}_\theta \otimes \mathbf{e}_\theta + \lambda \mathbf{e}_z \otimes \mathbf{e}_z, \quad (2.12)$$

where  $\lambda$  is the constant stretch in the axial direction, and  $\{\mathbf{e}_r, \mathbf{e}_\theta, \mathbf{e}_z\}$  are the usual basis vectors for cylindrical polar coordinates. The principal axes of stretch coincide with the coordinate axes. Let the  $z$ -,  $r$ - and  $\theta$ -directions be the 1-, 2- and 3-directions. The three principal stretches are  $\lambda_1 = \lambda$ ,  $\lambda_2 = \lambda_3 = 1/\sqrt{\lambda}$ . As a result, the elastic moduli enjoy the following properties which we use frequently:

$$\mathcal{A}_{2121} - \mathcal{A}_{2112} = \bar{p}, \quad \mathcal{A}_{3131} - \mathcal{A}_{3113} = \bar{p}, \quad \mathcal{A}_{1122} = \mathcal{A}_{1133}, \quad \mathcal{A}_{2222} = \mathcal{A}_{3333} \text{ etc.} \quad (2.13)$$

Our aim is to determine the critical value of  $\lambda$ , denoted  $\lambda_{\text{cr}}$ , at which localized necking takes place, and the necking profile when  $\lambda$  varies in a small neighbourhood of this critical value. We observe that since the material and the primary deformation (2.12) are both assumed to be homogeneous, our analysis cannot predict the location of the necking although we shall assume without loss of generality that the center of necking is located at  $Z = 0$ . In real applications the location is determined by the inevitable geometrical imperfections or material inhomogeneities.

Anticipating that the necking deformation under consideration is axi-symmetric, we consider  $\mathbf{u}$  in the form

$$\mathbf{u} = u(r, z)\mathbf{e}_r + v(r, z)\mathbf{e}_z, \quad (2.14)$$

where  $u(r, z)$  and  $v(r, z)$  denote the incremental displacement in the  $r$ - and  $z$ -directions, respectively. It then follows that

$$\eta = \text{grad } \mathbf{u} = u_r \mathbf{e}_r \otimes \mathbf{e}_r + u_z \mathbf{e}_r \otimes \mathbf{e}_z + v_r \mathbf{e}_z \otimes \mathbf{e}_r + v_z \mathbf{e}_z \otimes \mathbf{e}_z + \frac{u}{r} \mathbf{e}_\theta \otimes \mathbf{e}_\theta, \quad (2.15)$$

where  $u_r = \partial u / \partial r$ ,  $u_z = \partial u / \partial z$  etc. The equilibrium equations that are not satisfied automatically are

$$\chi_{2j,j} + \frac{1}{r}(\chi_{22} - \chi_{33}) = 0, \quad \chi_{1j,j} + \frac{1}{r}\chi_{12} = 0. \quad (2.16)$$

They will be subjected to the manipulation given by (2.11); for instance, the second equation will be replaced by

$$l_2 \equiv \chi_{1j,j} - (\bar{p} + p^*)\xi_{j1,j} + \frac{1}{r}\chi_{12} - \frac{1}{r}(\bar{p} + p^*)\xi_{21} = 0. \quad (2.17)$$

These equations are augmented by the incompressibility condition which can be expanded as

$$\eta_{ii} - \frac{1}{2}\eta_{mn}\eta_{nm} + \dots = 0. \quad (2.18)$$

We also need to expand the boundary conditions to quadratic order. The external surface of the tube is assumed to be traction-free, and so we have

$$\chi_{i2} = 0, \quad r = a. \quad (2.19)$$

For numerical illustrations, we shall assume that the strain-energy function is given by

$$W = \frac{2\mu}{m^2}(\lambda_1^m + \lambda_2^m + \lambda_3^m - 3) \quad (2.20)$$

with  $m = 1/2$ , where  $\mu$  is the ground state shear modulus. We shall scale all lengths by  $A$ , stress and  $W$  by  $\mu$ , and use the same symbols to denote the scaled quantities. Therefore, from now on we have  $\mu = 1$  and  $A = 1$ . All of our symbolic manipulations and numerical integrations are carried out with the aid of Mathematica (Wolfram Research Inc, 2019).

### 3. Near-critical necking solution

We first assume that the cylinder is infinitely long, and look for an asymptotic solution for (2.11) and (2.18) subject to the boundary conditions (2.19). We use  $\lambda$  as the control parameter in our post-bifurcation analysis, and write

$$\lambda = \lambda_{\text{cr}} + \varepsilon\lambda_0, \quad (3.1)$$

where  $\lambda_0$  is a constant and  $\varepsilon$  is a small positive parameter characterizing the order of deviation of  $\lambda$  from its critical value  $\lambda_{\text{cr}}$ . We expect that the necking solution that we are looking for is localized but slowly varying in the  $z$ -direction, depending on  $z$  through the far distance variable  $s$  defined by (Fu, 2001)

$$s = \sqrt{\varepsilon}z. \quad (3.2)$$

Note that as a result of (3.1), all the elastic moduli and other quantities that depend on  $\lambda$  should also be expanded into Taylor series around  $\lambda = \lambda_{\text{cr}}$ . For instance,

$$\mathcal{A}_{jilk} = \mathcal{A}_{jilk}^{(1)} + \varepsilon\lambda_0\mathcal{A}'_{jilk} + \dots, \quad a = a_0 + \varepsilon\lambda_0a_1 + \dots, \quad (3.3)$$

where  $\mathcal{A}'_{jilk}$  denotes the derivative of  $\mathcal{A}_{jilk}$  with respect to  $\lambda$  evaluated at  $\lambda = \lambda_{\text{cr}}$ , and the constants  $a_0$  and  $a_1$  are given by  $a_0 = \lambda_{\text{cr}}^{-1/2}$ ,  $a_1 = -\lambda_0a_0/(2\lambda_{\text{cr}})$ . In our subsequent analysis, we use  $\mathcal{A}_{jilk}$  to denote  $\mathcal{A}_{jilk}^{(1)}$  to simplify notation, and the second-order moduli  $\mathcal{A}_{jilknm}^2$  are all evaluated at  $\lambda = \lambda_{\text{cr}}$  whenever they appear.

Guided by the scalings given by Fu (2001), we deduce that  $u = O(\sqrt{\varepsilon}v)$ ,  $p^* = O(\sqrt{\varepsilon}v)$ , and that  $v$  is of order  $\sqrt{\varepsilon}$ . Thus, we look for an asymptotic solution of the form

$$\begin{aligned} u &= \varepsilon \{ u^{(1)}(r, s) + \varepsilon u^{(2)}(r, s) + \varepsilon^2 u^{(3)}(r, s) + \dots \}, \\ v &= \sqrt{\varepsilon} \{ v^{(1)}(r, s) + \varepsilon v^{(2)}(r, s) + \varepsilon^2 v^{(3)}(r, s) + \dots \}, \\ p^* &= \varepsilon \{ p^{(1)}(r, s) + \varepsilon p^{(2)}(r, s) + \varepsilon^2 p^{(3)}(r, s) + \dots \}, \end{aligned} \quad (3.4)$$

where all the functions on the right hand sides are to be determined from successive approximations.

In the linear analysis, the incremental pressure  $p^*$  can be eliminated by replacing the two equilibrium equations  $l_1 = 0, l_2 = 0$  by  $l_{1,2} - l_{2,1} = 0$ , where  $l_1$  and  $l_2$  are defined by (2.11). In the current nonlinear setting, it is no longer possible to eliminate  $p^*$  completely, but nonetheless through this manipulation  $p^*$  does not appear at first- and second-orders.

On substituting (3.4) into  $l_{1,2} - l_{2,1} = 0$ , the incompressibility condition (2.18), the boundary conditions (2.19), and then equating the coefficients of like powers of  $\varepsilon$ , we obtain a hierarchy of boundary value problems. To leading order, we obtain

$$\frac{d}{dr} \frac{1}{r} \frac{d}{dr} r v_{rs}^{(1)} = 0, \quad v_s^{(1)} + \frac{1}{r} \frac{d}{dr} r u^{(1)} = 0, \quad 0 < r < a_0, \quad (3.5)$$

and

$$v_{rs}^{(1)} = 0, \quad \frac{1}{r} \frac{d}{dr} r v_{rs}^{(1)} = 0, \quad \text{on } r = a_0, \quad (3.6)$$

where  $v_s^{(1)} = \partial v^{(1)} / \partial s$  and  $v_{rs}^{(1)} = \partial^2 v^{(1)} / \partial r \partial s$ .

Using (3.5)<sub>2</sub> to eliminate  $v_s^{(1)}$  from (3.5)<sub>1</sub> and (3.6), we obtain

$$\mathcal{L}[u^{(1)}] = 0, \quad 0 < r < a_0, \quad (3.7)$$

$$\mathcal{B}_1[u^{(1)}] = 0, \quad \mathcal{B}_2[u^{(1)}] = 0, \quad \text{on } r = a_0, \quad (3.8)$$

where the three differential operators are defined by

$$\mathcal{L}[u] = \frac{d}{dr} \frac{1}{r} \frac{d}{dr} r \frac{d}{dr} \frac{1}{r} \frac{d}{dr} r u, \quad \mathcal{B}_1[u] = \frac{1}{r} \frac{d}{dr} r \frac{d}{dr} \frac{1}{r} \frac{d}{dr} r u, \quad \mathcal{B}_2[u] = \frac{d}{dr} \frac{1}{r} \frac{d}{dr} r u.$$

The three operators satisfy the identity (Ye et al., 2020)

$$\int_0^{a_0} \{r g \mathcal{L}[f] - r f \mathcal{L}[g]\} dr = \{r g \mathcal{B}_1[f] - r f \mathcal{B}_1[g] + (r f)' \mathcal{B}_2[g] - (r g)' \mathcal{B}_2[f]\} \Big|_0^{a_0}, \quad (3.9)$$

where  $f$  and  $g$  are any two sufficiently smooth functions. This identity will be used to derive the amplitude equation later.

On integrating (3.5), we find that  $v_1^{(1)}$  and  $u_1^{(1)}$  must be a linear combination of the independent solutions

$$1, \quad r^2, \quad \log(r),$$

and

$$r, \quad r^3, \quad r \log(r), \quad \frac{1}{r},$$

respectively. However, on substituting this general solution into the boundary conditions (3.6) and noting that the solution must be bounded at  $r = 0$ , we find that  $u^{(1)}$  and  $v^{(1)}$  take the reduced form

$$v^{(1)} = -A_1(s), \quad u^{(1)} = c_1(s)r, \quad (3.10)$$

where  $c_1(s)$  is an arbitrary function, and  $A_1'(s) = 2c_1(s)$ .

At second order, we find that  $u^{(2)}$  and  $v^{(2)}$  satisfy the governing equations

$$\frac{d}{dr} \frac{1}{r} \frac{d}{dr} r v_{rs}^{(2)} = 0, \quad v_s^{(2)} + \frac{1}{r} \frac{d}{dr} r u_1^{(2)} = 3c_1^2(s), \quad 0 < r < a_0, \quad (3.11)$$

and boundary conditions

$$v_{rs}^{(2)} = -r c_1''(s), \quad \zeta_1 \frac{1}{r} \frac{d}{dr} r v_{rs}^{(2)} = \zeta_2 c_1''(s), \quad \text{on } r = a_0, \quad (3.12)$$

where the constants  $\zeta_1$  and  $\zeta_2$  are defined by

$$\zeta_1 = \mathcal{A}_{2121}, \quad \zeta_2 = \mathcal{A}_{2121} + \mathcal{A}_{3333} - 4\mathcal{A}_{1133} + \mathcal{A}_{2233} + 2\mathcal{A}_{1111} - 3\mathcal{A}_{2112}. \quad (3.13)$$

Equations (3.11) can be solved to give

$$v^{(2)} = -2 \int c_2(s) ds + \frac{1}{2} A_2(s) r^2, \quad u^{(2)} = \frac{3}{2} r c_1^2(s) + r c_2(s) - \frac{1}{8} r^3 A_2'(s), \quad (3.14)$$

where  $c_2(s)$  and  $A_2(s)$  are functions to be determined. On substituting (3.14)<sub>1</sub> into the boundary conditions (3.12), we obtain

$$c_1''(s) + A_2'(s) = 0, \quad \zeta_2 c_1''(s) - 2\zeta_1 A_2'(s) = 0. \quad (3.15)$$

It then follows that a non-trivial solution exists only if the following bifurcation condition is satisfied:

$$2\zeta_1 + \zeta_2 = 0. \quad (3.16)$$

We now show that this bifurcation condition has a clear physical interpretation. To this end, we note that

$$\sigma_{11} = \lambda_1 W_1 - p, \quad \sigma_{22} = \lambda_2 W_2 - p,$$

where  $W_1 = \partial W / \partial \lambda_1$ ,  $W_2 = \partial W / \partial \lambda_2$ . Solving  $\sigma_{22} = 0$  for  $p$ , we obtain

$$\sigma_{11} = \lambda_1 W_1 - \lambda_2 W_2 = \lambda W_1 - \lambda^{-1/2} W_2 = \lambda w'(\lambda),$$

where

$$w(\lambda) = W(\lambda, \lambda^{-1/2}, \lambda^{-1/2}). \quad (3.17)$$

The nominal stress in the axial direction is  $\lambda^{-1} \sigma_{11} = w'(\lambda)$ . The bifurcation (3.16) is then identical to  $w''(\lambda) = 0$ , which means that bifurcation takes place when the axial nominal stress reaches a maximum.

Once  $u^{(1)}$ ,  $v^{(1)}$  and  $v^{(2)}$  are known, the leading order incremental pressure  $p^{(1)}$  can be obtained by equating the coefficients of  $\varepsilon^{3/2}$  in (2.16)<sub>2</sub> and then integrating the resulting equation with respect to  $s$ . We thus obtain

$$p^{(1)} = (\mathcal{A}_{1133} - 2\mathcal{A}_{1111} + \mathcal{A}_{1122} + 2\mathcal{A}_{2112}) c_1(s) + 2\zeta_1 \int^s A_2(s) ds. \quad (3.18)$$

We now have all the solutions to derive the amplitude equation.

At third order, we obtain

$$\mathcal{L}[u^{(3)}] = k_1 r c_1^{(4)}, \quad (3.19)$$

where

$$k_1 = \zeta_1^{-1} (2\mathcal{A}_{1133} + 2\mathcal{A}_{1221} - \mathcal{A}_{3333} - \mathcal{A}_{1111} - \mathcal{A}_{1212}).$$

The boundary conditions take the form

$$\mathcal{B}_1[u^{(3)}] = k_2 r^2 c_1'''' + k_3 \lambda_0 c_1'' + k_4 (c_1')^2 + (k_4 - 10) c_1 c_1'' + k_5 c_2'', \quad (3.20)$$



$$\mathcal{B}_2[u^{(3)}] = k_6 r^3 c_1'''' + k_7 \lambda_0 c_1'' + k_8 r (c_1')^2 + r(k_8 - 5)c_1 c_1'' + r k_9 c_2'', \quad (3.21)$$

where  $k_2, \dots, k_9$  are constants whose expressions are not written out here for the sake of brevity.

Since the homogeneous form of the above boundary value problem has a non-trivial solution, the nonhomogeneous terms on the right hand sides of the three equations (3.19), (3.20) and (3.21) must satisfy a solvability condition. This condition may be obtained by taking  $f = u^{(3)}$ , and  $g$  to be any solution of the leading-order problem, e.g.  $g = r$ , in the identity (3.9). This gives

$$\int_0^{a_0} r^2 \mathcal{L}[u^{(3)}] dr = (r^2 \mathcal{B}_1[u^{(3)}] - 2r \mathcal{B}_2[u^{(3)}])|_0^{a_0}. \quad (3.22)$$

On evaluating the integral and simplifying, we obtain the amplitude equation

$$d_1 c_1''''(s) + \lambda_0 d_2 c_1''(s) + \frac{1}{2} d_3 (c_1^2(s))'' = 0, \quad (3.23)$$

where  $d_1$ ,  $d_2$  and  $d_3$  are given by

$$\begin{aligned} d_1 &= \frac{1}{8} a_0^2 \{ \mathcal{A}_{3333} - 4\mathcal{A}_{1133} + \mathcal{A}_{2233} + 2\mathcal{A}_{1111} - 2\mathcal{A}_{1212} - 3\mathcal{A}_{1221} + 5\mathcal{A}_{2121} \}, \\ d_2 &= \mathcal{A}'_{3333} - 4\mathcal{A}'_{1133} + B'_{2233} + 2\mathcal{A}'_{1111} - 3\mathcal{A}'_{2112} + 3\mathcal{A}'_{2121}, \\ d_3 &= 3\mathcal{A}_{3333} + 6\mathcal{A}_{1133} + 3\mathcal{A}_{2233} - 12\mathcal{A}_{1111} + 3\mathcal{A}_{2112} - 3\mathcal{A}_{2121} + \mathcal{A}_{333333}^2 \\ &\quad - 6\mathcal{A}_{113333}^2 + 3\mathcal{A}_{223333}^2 + 12\mathcal{A}_{331111}^2 - 6\mathcal{A}_{331122}^2 - 4\mathcal{A}_{111111}^2. \end{aligned}$$

Focusing on localized solutions that satisfy the decay conditions  $c_1(s) \rightarrow 0$  as  $s \rightarrow \pm\infty$ , we may integrate (3.23) twice to obtain

$$d_1 c_1''(s) + \lambda_0 d_2 c_1(s) + \frac{1}{2} d_3 c_1^2(s) = 0. \quad (3.24)$$

Collecting all the results obtained so far, we find that  $F$  takes the form

$$\begin{bmatrix} \lambda(1 - 2\varepsilon c_1(s)) + O(\varepsilon^2) & O(\varepsilon^{3/2}) & 0 \\ O(\varepsilon^{3/2}) & \lambda^{-1/2}(1 + \varepsilon c_1(s)) + O(\varepsilon^{3/2}) & 0 \\ 0 & 0 & \lambda^{-1/2}(1 + \varepsilon c_1(s)) + O(\varepsilon^{3/2}) \end{bmatrix}.$$

This shows that even to order  $\varepsilon$ , the principal axes still coincide with the three coordinate axes, and the principal stretch to order  $\varepsilon$  in the axial direction is given by

$$\lambda_1 = \lambda(1 - 2\varepsilon c_1(s)) = \lambda_{\text{cr}} + \varepsilon \lambda_0 - 2\varepsilon c_1(s) \lambda_{\text{cr}} + O(\varepsilon^2). \quad (3.25)$$

Since the nominal stress attains its maximum at  $\lambda = \lambda_{\text{cr}}$ , the local behaviour of stress versus  $\lambda$  in a small neighbourhood of  $\lambda = \lambda_{\text{cr}}$  must be parabolic. This means that if  $c_1(s)$  is a

constant the principal stretch given by (3.25) and the stretch  $\lambda_{\text{cr}} + \varepsilon\lambda_0$  must lie on opposite sides of, and be equi-distance from,  $\lambda = \lambda_{\text{cr}}$ , that is,

$$\lambda_{\text{cr}} + \varepsilon\lambda_0 + (\lambda_{\text{cr}} + \varepsilon\lambda_0 - 2\varepsilon c_1(s)\lambda_{\text{cr}}) = 2\lambda_{\text{cr}},$$

from which we obtain  $c_1(s) = \lambda_0/\lambda_{\text{cr}}$ . On substituting this constant solution into (3.24), we obtain  $d_3 = -2\lambda_{\text{cr}}d_2$  which provides a useful check on our derivations. As a result, the amplitude equation may be reduced to

$$d_1 c_1''(s) + d_2 (\lambda_0 c_1(s) - \lambda_{\text{cr}} c_1^2(s)) = 0. \quad (3.26)$$

Finally, we observe that once  $c_1(s)$  is determined the radius of the necked cylinder is given by

$$r(a) = a_0 + \varepsilon\lambda_0 a_1 + \varepsilon a_0 c_1(s) + \dots. \quad (3.27)$$

#### 4. Connection with the 1D model of Audoly and Hutchinson (2016)

We first summarize the theory proposed by Audoly and Hutchinson (2016) for a *compressible* cylinder of arbitrary cross-section, and then specialize to the case of an *incompressible* cylinder of circular cross-section. The position vector corresponding to a uni-axial tension in the axial direction for a compressible cylinder is given by

$$\mathbf{x} = \lambda Z \mathbf{e}_z + \mu(\lambda)(X_2 \mathbf{e}_2 + X_3 \mathbf{e}_3), \quad (4.1)$$

where  $\mathbf{e}_2$  and  $\mathbf{e}_3$  together with  $\mathbf{e}_z$  are unit vectors associated with a rectangular coordinate system,  $X_1(\equiv Z)$ ,  $X_2$  and  $X_3$  are the associated coordinates of  $\mathbf{X}$ , the  $\lambda$  has the same meaning as in the previous sections and  $\mu(\lambda)$  is the stretch in the transverse directions which is determined by  $\sigma_{22} = 0$  (where  $\sigma$  is the Cauchy stress). To describe necking solutions, Coleman & Newman (1988) replaced the constant stretch  $\lambda$  by a function  $\lambda(Z)$ , and (4.1) by

$$\mathbf{x} = \Lambda(Z) \mathbf{e}_1 + \mu(\lambda(Z))(X_2 \mathbf{e}_2 + X_3 \mathbf{e}_3),$$

where  $\Lambda(Z)$  is defined by  $\Lambda'(Z) = \lambda(Z)$ . Not surprisingly, this representation is not expected to be asymptotically self-consistent in the sense among terms of the same order, some terms are kept in the analysis whereas others are not. The correct expansion is of the form (Audoly & Hutchinson, 2016)

$$\begin{aligned} x_1 &= \Lambda(Z) + (X_2^2 + X_3^2 - K)v_1(Z) + \dots, \\ x_2 &= \mu(\lambda(Z))X_2 + \dots, \\ x_3 &= \mu(\lambda(Z))X_3 + \dots, \end{aligned} \quad (4.2)$$

where the function  $v_1(Z)$  is to be determined, and  $K$  is a normalization constant such that the area integral of  $X_2^2 + X_3^2 - K$  over the cross section vanishes. This representation is simply a Taylor expansion of the displacement field in terms of the transverse coordinates  $X_2$  and  $X_3$  by taking into account the fact that for the current necking problem, the axial displacement must be an even function of  $X_2$  and  $X_3$ , whereas the other two displacement components must be odd functions of  $X_2$  and  $X_3$ , respectively. Thus the omitted terms in  $x_1$  must be at least quartic in  $X_2$  and  $X_3$ , whereas the omitted terms in  $x_2$  and  $x_3$  must be at least cubic in  $X_2$  and  $X_3$ . As a result, these omitted terms are not involved in the following analysis, but the term containing  $v_1$  will. The term  $X_2^2 + X_3^2$  in  $x_1$  could be replaced by  $kX_2^2 + X_3^2$  with  $k$  a constant, but energy minimization would eventually give  $k = 1$ . We note that Dai et al. (2008) and Dai & Peng (2012) proposed similar expansions to characterize necking, but their expansions were around a *uniform* finite deformation.

To keep track of the orders of different terms, we may define two scaled coordinates and scale  $K$  through

$$(\bar{X}_2, \bar{X}_3, \bar{K}) = \frac{1}{\varepsilon}(X_2, X_3, K),$$

where  $\varepsilon$  is a small positive parameter not related to the  $\varepsilon$  in the previous sections. Corresponding to (4.2) the deformation gradient takes the form

$$F = (I + \varepsilon V^{(1)} + \varepsilon^2 V^{(2)} + \dots)F_0,$$

where

$$F_0 = \begin{bmatrix} \lambda(Z) & 0 & 0 \\ 0 & \mu(\lambda) & 0 \\ 0 & 0 & \mu(\lambda) \end{bmatrix}, \quad V^{(1)} = \begin{bmatrix} 0 & q_2 & q_3 \\ p_2 & 0 & 0 \\ p_3 & 0 & 0 \end{bmatrix},$$

$$V^{(2)} = \begin{bmatrix} \lambda^{-1}(\bar{X}_2^2 + \bar{X}_3^2 - \bar{K})v_1'(Z) & 0 & 0 \\ 0 & * & * \\ 0 & * & * \end{bmatrix}.$$

In the above expressions, the  $p$ 's and  $q$ 's are given by

$$p_2 = \lambda^{-1}t\bar{X}_2, \quad p_3 = \lambda^{-1}t\bar{X}_3, \quad q_2 = 2\mu^{-1}\bar{X}_2v_1(Z), \quad q_3 = 2\mu^{-1}\bar{X}_3v_1(Z),$$

with  $t$  defined by  $t(Z) = d\mu/dZ$ , and the  $*$ 's denote non-zero components that are not needed in the subsequent analysis.

On expanding the strain-energy function around  $F = F_0$ , we obtain

$$W = W(F_0) + J\sigma_{ij}(\varepsilon V_{ij}^{(1)} + \varepsilon^2 V_{ij}^{(2)}) + \frac{1}{2}J\mathcal{A}_{jilk}V_{ij}^{(1)}V_{kl}^{(1)} + O(\varepsilon^3), \quad (4.3)$$

where  $J = \det F_0$ ,  $(\sigma_{ij})$  is the Cauchy stress associated with the deformation gradient  $F_0$ , and the instantaneous elastic moduli  $\mathcal{A}_{jilk}$  are given by (2.10) with  $\bar{F}$  replaced by  $F_0$ . With

the use of the facts that corresponding to  $F_0$  the principal axes of stretch coincide with the coordinate axes and the deformation is due to a uni-axial tension so that  $\sigma_{22} = \sigma_{33} = 0$ , equation (4.3) can be reduced to

$$W = W(F_0) + \varepsilon^2 J \sigma_{11} \lambda^{-1} (\bar{X}_2^2 + \bar{X}_3^2 - \bar{K}) v_1'(Z) + \frac{1}{2} \varepsilon^2 J \{ \mathcal{A}_{2121} (q_2 + p_2)^2 + \mathcal{A}_{3131} (p_3 + q_3)^2 + \sigma_{11} (p_2^2 + p_3^2) \} + O(\varepsilon^3), \quad (4.4)$$

where we have also made use of the facts that for compressible materials

$$\mathcal{A}_{2121} - \mathcal{A}_{2112} \equiv \sigma_{22} = 0, \quad \mathcal{A}_{3131} - \mathcal{A}_{3113} \equiv \sigma_{33} = 0, \quad \mathcal{A}_{1212} - \mathcal{A}_{2121} \equiv \sigma_{11} - \sigma_{22} = \sigma_{11},$$

and  $\mathcal{A}_{1313} = \mathcal{A}_{1212}$  etc. It is then seen that energy is minimized by choosing  $v_1$  to satisfy  $q_2 + p_2 = 0$ ,  $q_3 + p_3 = 0$ . As a result, equation (4.4) reduces to

$$W = W(F_0) + \varepsilon^2 n(\lambda) (\bar{X}_2^2 + \bar{X}_3^2 - \bar{K}) v_1'(Z) + \frac{1}{2} \varepsilon^2 n(\lambda) \lambda^{-1} t^2 (\bar{X}_2^2 + \bar{X}_3^2) + O(\varepsilon^3), \quad (4.5)$$

where  $n(\lambda)$  ( $= J \lambda^{-1} \sigma_{11} = w'(\lambda)$ ) is the nominal stress in the axial direction.

When the above expression is integrated over the cross section, the term involving  $v_1'(Z)$  vanishes. The integral of  $\varepsilon^2 (\bar{X}_2^2 + \bar{X}_3^2)$  is the geometric moment of inertia of the cross-section which we denote by  $M$ . We then have

$$\mathcal{E}[\lambda] = \int_{B_0} W(F) dZ dX_2 dX_3 = \int_{-L}^L \left\{ S W(F_0) + \frac{M}{2} n(\lambda) \lambda^{-1} t^2 \right\} dZ, \quad (4.6)$$

where  $S$  is the cross-sectional area. This is the equation (2.28a) of Audoly & Hutchinson (2016).

Specializing the above expression to an incompressible circular cylinder for which  $\mu = \lambda^{-1/2}$  so that  $t = -\lambda^{-3/2} \lambda'(Z)/2$ , we obtain

$$\mathcal{E}[\lambda] = \int_{B_0} W(F) dZ dX_2 dX_3 = \pi \int_{-L}^L \{ w(\lambda) + 2b(\lambda) (\lambda')^2 \} dZ, \quad (4.7)$$

where  $w(\lambda)$  is given by (3.17), and  $b(\lambda)$  is defined by

$$b(\lambda) = \frac{n(\lambda)}{32\lambda^4}. \quad (4.8)$$

Suppose now that the cylinder is stretched by a force  $F$  per unit area in the reference configuration, then the total energy is

$$\pi \int_{-L}^L \{ w(\lambda) + 2b(\lambda) (\lambda')^2 - F \lambda \} dZ.$$

The associated Euler-Lagrangian equation is

$$w'(\lambda) + 2b'(\lambda) (\lambda')^2 - F - \frac{d}{dX} (4b(\lambda) \lambda') = 0,$$

or equivalently,

$$w'(\lambda) - 4b(\lambda)\lambda'' - 2b'(\lambda)(\lambda')^2 - F = 0. \quad (4.9)$$

This has an integral given by

$$w(\lambda) - 2b(\lambda)(\lambda')^2 - F\lambda = C. \quad (4.10)$$

This concludes our summary of the 1D theory of Audoly & Hutchinson (2016), and from this point onwards our analysis deviates from theirs since our aim is to determine the range of validity when the finite-length cylinder is treated effectively as an infinite cylinder.

Focusing on localized solutions in an infinitely long cylinder, and denoting the limiting value of  $\lambda$  as  $Z \rightarrow \pm\infty$  by  $\lambda_\infty$ , we have  $F = n(\lambda_\infty) = w'(\lambda_\infty)$  and from (4.10)

$$w(\lambda) - 2b(\lambda)(\lambda')^2 - w'(\lambda_\infty)\lambda = w(\lambda_\infty) - w'(\lambda_\infty)\lambda_\infty. \quad (4.11)$$

Following Fu et al. (2008), we now look for a bifurcation solution given by

$$\lambda = \lambda_\infty + y(Z), \quad (4.12)$$

where  $y(Z)$  is a perturbation from the uniform solution. It then follows that

$$\frac{1}{2}w''(\lambda_\infty)y^2 + \frac{1}{6}w'''(\lambda_\infty)y^3 - 2b(\lambda_\infty)(y')^2 = O(y^4).$$

On differentiating once and neglecting higher order terms, we obtain

$$4b(\lambda_\infty)y'' = w''(\lambda_\infty)y + \frac{1}{2}w'''(\lambda_\infty)y^2. \quad (4.13)$$

Solutions of the linearized version of this equation change character when the sign of  $w''(\lambda_\infty)$  changes. Thus, the bifurcation condition is given by  $w''(\lambda_\infty) = 0$  which is equivalent to (3.16). Denote the first root of this equation by  $\lambda_{\text{cr}}$ . Then in a small neighbourhood of this point, the amplitude equation is

$$4b(\lambda_{\text{cr}})y'' = w'''(\lambda_{\text{cr}})(\lambda_\infty - \lambda_{\text{cr}})y + \frac{1}{2}w'''(\lambda_{\text{cr}})y^2, \quad (4.14)$$

which is identical to the equation (6.12) of Dai & Peng (2012) when specialized to the particular compressible material model considered by the latter authors. The above equation does indeed have a localized solution given by

$$y(Z) = -3(\lambda_\infty - \lambda_{\text{cr}}) \operatorname{sech}^2 \left[ \frac{1}{4} \sqrt{\frac{w'''(\lambda_{\text{cr}})(\lambda_\infty - \lambda_{\text{cr}})}{b(\lambda_{\text{cr}})}} Z \right]. \quad (4.15)$$

This solution is valid when  $w'''(\lambda_{\text{cr}})(\lambda_\infty - \lambda_{\text{cr}}) > 0$ . Since the bifurcation point corresponds to the maximum of the nominal stress, we have  $w'''(\lambda_{\text{cr}}) < 0$ . It then follows that the

bifurcation is always subcritical (i.e.  $\lambda_\infty - \lambda_{\text{cr}} < 0$ ) and the bifurcated solution corresponds to a localized reduction in the radius. The axial stretch at  $Z = 0$  is given by

$$\lambda(0) = \lambda_\infty - 3(\lambda_\infty - \lambda_{\text{cr}}) = 3\lambda_{\text{cr}} - 2\lambda_\infty. \quad (4.16)$$

To compare the amplitude equation (3.26) with the above 1D theory, we note that  $a_0 = \lambda_{\text{cr}}^{-1/2}$ , and

$$y' = \frac{dy}{dZ} = \frac{dy}{dz} \frac{dz}{dZ} = \lambda_{\text{cr}} \frac{dy}{dz}, \quad y'' = \lambda_{\text{cr}}^2 \frac{d^2y}{dz^2}.$$

Equation (4.14) then becomes

$$4\lambda_{\text{cr}}^2 b(\lambda_{\text{cr}}) y'' = w'''(\lambda_{\text{cr}}) (\lambda_\infty - \lambda_{\text{cr}}) y + \frac{1}{2} w'''(\lambda_{\text{cr}}) y^2. \quad (4.17)$$

Comparing (4.12) with (3.25) shows that  $y = -2c_1(s)\lambda_{\text{cr}}\varepsilon$ . In terms of  $c_1(s)$ , the amplitude equation (4.17) becomes

$$4\lambda_{\text{cr}}^2 b(\lambda_{\text{cr}}) c_1''(s) = w'''(\lambda_{\text{cr}}) [\lambda_0 c_1(s) - \lambda_{\text{cr}} c_1^2(s)]. \quad (4.18)$$

This is identical to (3.26) provided

$$\frac{w'''(\lambda_{\text{cr}})}{4\lambda_{\text{cr}}^2 b(\lambda_{\text{cr}})} = -\frac{d_2}{d_1}.$$

We have checked and verified that this is indeed the case.

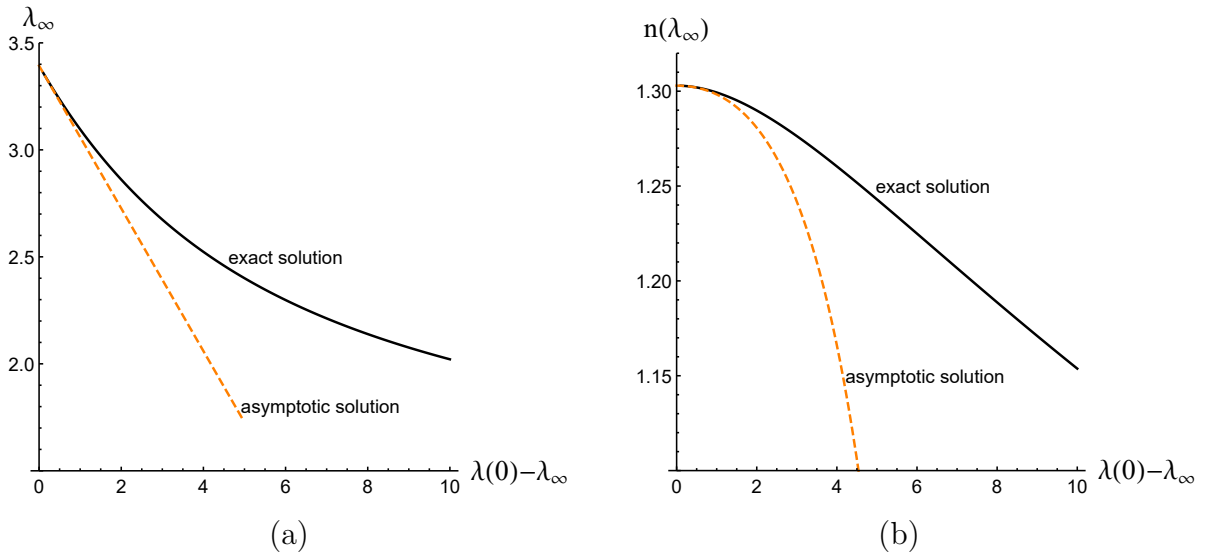


Figure 1: Dependence of  $\lambda_\infty$  (left) and the nominal stress  $n(\lambda_\infty)$  (right) on the necking amplitude “ $\lambda(0) - \lambda_\infty$ ” corresponding to an infinitely long cylinder with the constitutive behaviour described by (2.20). Results for the power-law model are very similar except that the critical value of  $\lambda_\infty$  is smaller.

## 5. Effects of finite length and validity of the infinite-length assumption

Return now to the fully nonlinear equation (4.9). We shall determine the variation of  $\lambda(0)$  with respect to  $\lambda(L)$  in the fully nonlinear regime, and assess the effects of finite length. Note that  $\lambda(L)$  becomes  $\lambda_\infty$  and  $F$  becomes  $n(\lambda_\infty)$  when  $L$  is infinity.

We first consider the case when  $L$  is infinity. Evaluating (4.11) at  $Z = 0$  where  $\lambda' = 0$ , we obtain

$$w(\lambda(0)) - w'(\lambda_\infty)\lambda(0) = w(\lambda_\infty) - w'(\lambda_\infty)\lambda_\infty. \quad (5.1)$$

This defines  $\lambda(0)$  as a function of  $\lambda_\infty$ . The trivial solution  $\lambda(0) = \lambda_\infty$  is always a solution, but as  $\lambda_\infty$  reaches the critical value  $\lambda_{cr}$ , a non-trivial solution becomes possible. In Fig. 1, we have shown the variation of  $\lambda_\infty$  and nominal stress  $n(\lambda_\infty)$  against  $\lambda(0) - \lambda_\infty$  given by the fully nonlinear equation (5.1) and the leading-order asymptotic result (4.16). The strain energy function used is given by (2.20) with  $m = 1/2$ . As expected, the asymptotic result does capture the near-critical behaviour correctly. Corresponding to each non-trivial solution of  $\lambda(0)$ , the associated non-trivial solution for  $\lambda(Z)$  is obtained by integrating (4.9) subject to the “initial” data  $\lambda(0)$  and  $\lambda'(0)$  ( $= 0$ ). This solution automatically satisfies the decay condition  $\lambda \rightarrow 0$  as  $Z \rightarrow \infty$  since the initial data lie on the separatrix in the phase plane of the (spatial) dynamical system (4.9); see Fig. 2.

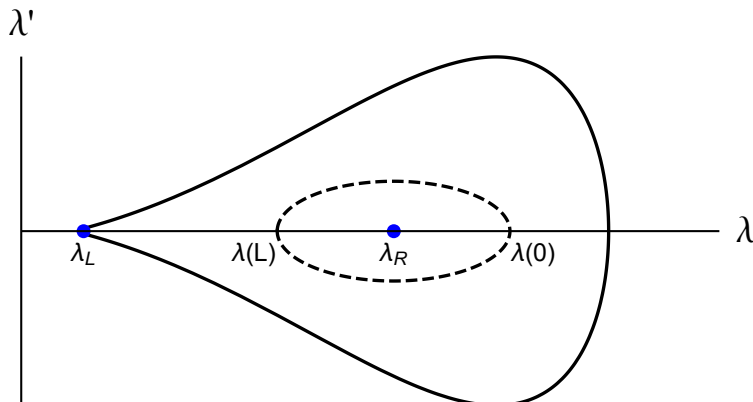


Figure 2: Phase portrait of the “spatial” dynamical system (4.9) showing the separatrix (solid line) and a typical closed orbit (dashed line).

In Audoly & Hutchinson (2016), the first-order differential equation (4.10) is solved subject to the “natural” boundary conditions  $\lambda'(0) = \lambda'(L) = 0$ . The solution is expressed in terms of an integral that is evaluated numerically, and results are presented for the plane-strain case with  $b(\lambda) = n(\lambda)/(12\lambda^5)$  and for the power law model

$$w(\lambda) = \frac{\sigma^*}{N+1} (\ln \lambda)^{N+1}, \quad (5.2)$$

where  $N$  ( $0 < N < 1$ ) and  $\sigma^*$  are material constants. Here we shall solve the original second-order differential equation (4.9) directly using a shooting method and assess the effects of different length/diameter ratios. We validate our numerical scheme by reproducing the results in Audoly & Hutchinson (2016) before computing the relevant results for a solid circular cylinder modelled by the strain-energy function (2.20). For the latter case, the load maximum determined by  $n'(\lambda) = w''(\lambda) = 0$  is given by  $F = F_{\max} \equiv 1.3029$  that is achieved when  $\lambda = \lambda_{\text{cr}} = 3.3930$  (recall that  $F$  has been scaled by  $\mu$ ). Necking solutions can only exist for  $F < F_{\max}$ . For each  $F < F_{\max}$ , equation (4.9) as a dynamical system has two fixed points, determined by  $n(\lambda) = F$  and denoted by  $\lambda_L$  and  $\lambda_R (> \lambda_L)$ , respectively. It can be shown that  $\lambda_L$  is a saddle, whereas  $\lambda_R$  is a center; see Fig. 2. As a result, there exists a single separatrix that starts and finishes at the saddle point. This separatrix represents a localized necking solution that can be approximated by (4.15) when  $F$  is sufficiently close to  $F_{\max}$ . Enclosed within the separatrix are an infinite number of closed orbits centered around  $\lambda_R$ . Each such orbit represents a periodic solution, and there exists exactly one such orbit corresponding to each  $L$  specified.

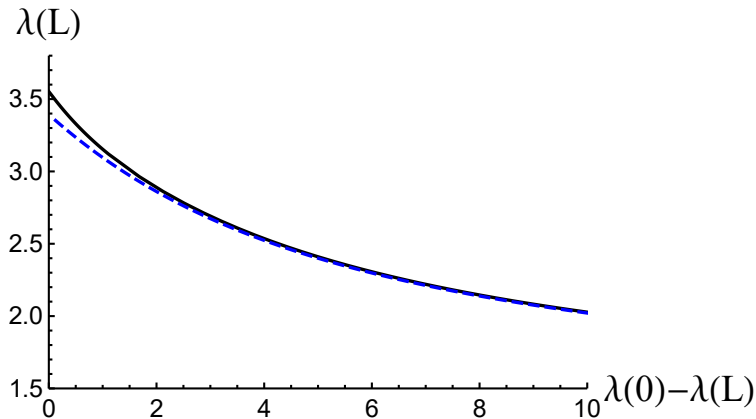


Figure 3: Solid line (black):  $\lambda_\infty$  against  $\lambda(0) - \lambda_\infty$  for an infinite cylinder ( $\lambda_\infty = \lambda(L)$ ). Dashed line (blue):  $\lambda(L)$  against  $\lambda(0) - \lambda(L)$  for a finite-length cylinder with  $L = 1$ . The two sets of results only differ near the bifurcation point where solution is not localized.

To determine the periodic solution for each specified  $L$ , we solve (4.9) numerically subject to the “initial” conditions

$$\lambda(0) = \lambda_0, \quad \lambda'(0) = 0, \quad (5.3)$$

where  $\lambda_0$  is to be found/tuned in order to satisfy the end condition  $\lambda'(L) = 0$ . Evaluating (4.10) at  $Z = 0$  and  $L$  in turn and then subtracting the two resulting equations to eliminate  $C$ , we obtain

$$F = \frac{w(\lambda_0) - w(\lambda(L))}{\lambda_0 - \lambda(L)}. \quad (5.4)$$



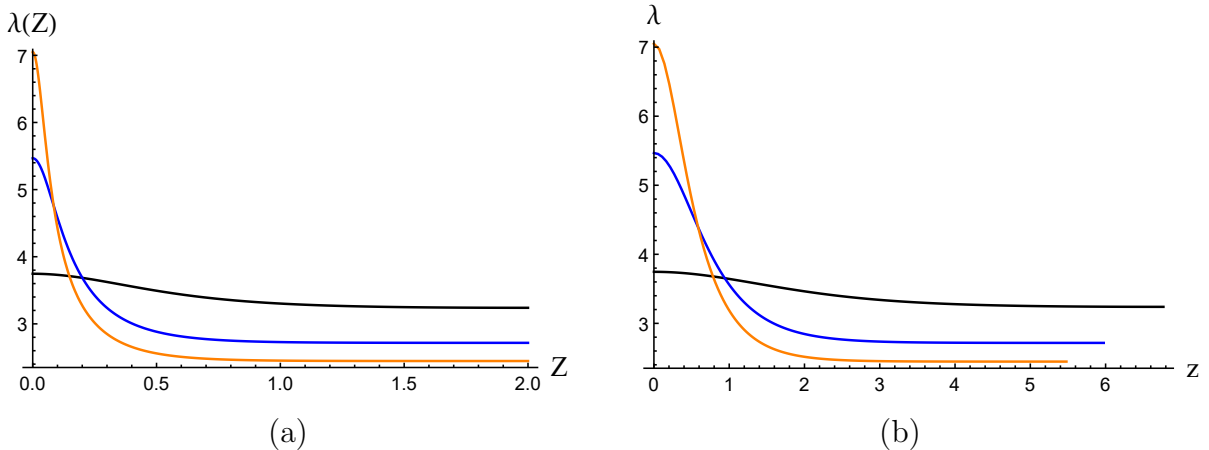


Figure 4: Profiles of the axial stretch  $\lambda$  as a function of  $Z$  (left) or  $z$  (right). The three profiles correspond to  $F = 1.3019$  (black), 1.2800 (blue), 1.2500 (orange), respectively, with lower values of  $F$  corresponding to larger values of  $\lambda(0)$  and more localized profiles.

It follows from the above description of the phase portrait that  $\lambda(L)$  must necessarily lie in the open interval  $(\lambda_L, \lambda_R)$ . It is this fact that makes our shooting procedure relatively straightforward. Our solution strategy is as follows. For each  $F < F_{\max}$ , we scan  $\lambda(L)$  in the interval  $(\lambda_L, \lambda_R)$ . For each  $\lambda(L)$ , the  $\lambda_0$  is determined by solving (5.4) and the equation (4.9) is then solved subject to (5.3) to find  $\lambda'(L)$ . If  $\lambda'(L)$  never changes sign when  $\lambda(L)$  reaches the right hand side  $\lambda_R$  of the interval, then the only solutions possible are the trivial solutions  $\lambda_0 = \lambda(L) = \lambda_R$  or  $\lambda_L$ ,  $F = n(\lambda_R) = n(\lambda_L)$ . Otherwise, a non-trivial solution exists and we iterate on  $\lambda(L)$  so that  $\lambda'(L)$  is less than a specified tolerance, say  $10^{-8}$ . For  $L < 2$ , our computation confirms the result of Audoly & Hutchinson (2016) that bifurcation takes place when

$$\frac{w''(\lambda)}{4b(\lambda)} + \frac{\pi^2}{L^2} = 0. \quad (5.5)$$

When  $L \geq 2$ , the above bifurcation condition can effectively be replaced by  $w''(\lambda) = 0$ , the bifurcation condition for an infinite cylinder. For instance, when  $L = 2$ ,  $\lambda_{\text{cr}}$  only differs from the exact bifurcation stretch by 1.2% and the associated axial forces for  $L = 2$  and  $L = \infty$  differ from each other by less than 0.005%.

We tried to superimpose the dependence of  $F$  on  $\lambda_0 - \lambda(L)$  for a finite cylinder on Fig. 1(b) that is for an infinite cylinder. It was found that the results for  $L \geq 1$  are all graphically indistinguishable from the solid curve shown in Fig. 1(b). We also tried to display the dependence of  $\lambda(L)$  on  $\lambda_0 - \lambda(L)$  in Fig. 1(a). For all  $L \geq 2$  the results are graphically indistinguishable from the solid curve in Fig. 1(a). Fig. 3 compares the two sets of results for the case  $L = 1$ . It is seen that even for this case the difference is only noticeable near the bifurcation point where the necking solution is less localized and so the end effect is indeed

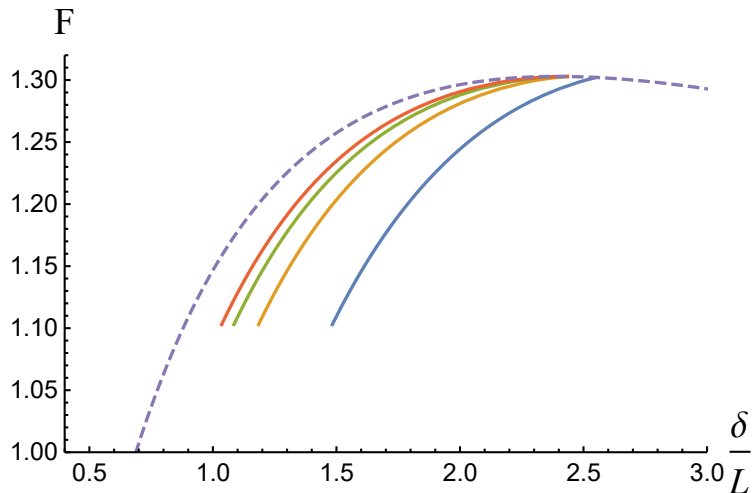


Figure 5: Variation of axial force against scaled end shortening (i.e. average strain) for  $L = 1, 2, 3, 4$  (solid lines), with snap-back more pronounced for larger values of  $L$ . The dashed line corresponds to the uniform solution.

significant. The above observations are surprising since we have expected the finite-length results to deviate from the result for an infinite cylinder at least for a very stubby cylinder such as the one with  $L = 2$ . To show why this is the case, we have shown in Fig. 4(a) the profiles of  $\lambda(Z)$  when  $L = 2$ , corresponding to  $F = 1.3019, 1.28$  and  $1.25$ , respectively. It is seen that even for  $F = 1.3019$  which is very close to  $F_{\max}$  and for which the solution is expected to spread over a large distance, the solution actually tends to  $\lambda(L)$  rapidly. Fig. 4(b) shows  $\lambda$  as a function of the current coordinate  $z$ . It is seen that the deformed lengths for lower values of  $F$  are shorter since the tube is stretched less.

The results shown in Fig. 4(a) highlight the difficulties that would arise when trying to satisfy the boundary condition  $\lambda'(L) = 0$  when  $L$  is large. Because each solution decays exponentially, the same solution would apply to cylinders of different lengths depending on the tolerance set, that is how accurately we satisfy this boundary condition. On the other hand, even if we fix the tolerance, by changing  $\lambda(0)$  by an infinitesimal amount we can satisfy  $\lambda'(L) = 0$  with different lengths. Therefore, when studying localized necking in a finite-length cylinder with natural boundary conditions, the cylinder can and should be treated as infinitely long even when the length/diameter ratio is as moderate as 2.

We now give further support to the above claim in a number of ways. Firstly, we show in Fig. 5 the variations of the axial force against end shortening  $\delta$  for four values of  $L$ . Assuming that cylinders with  $L = 3, 4$  can effectively be treated as infinite cylinders, we compute the corresponding  $\delta$  according to

$$\delta = \int_0^L \lambda(x) dx - L = \int_0^2 \lambda(x) dx - 2 + \int_2^L \lambda(2) dx - (L - 2) = \delta_2 + (\lambda(2) - 1)(L - 2), \quad (5.6)$$

where  $\delta_2$  is the end shortening associated with  $L = 2$  and  $\lambda(2)$  is calculated using the solution for  $L = 2$ . To verify the accuracy of this approximation, we repeat the same calculation for the energy function (5.2) and  $b(\lambda)$  adopted by Audoly & Hutchinson (2016), and find that the counterpart of our Fig. 5 exactly coincides with their Fig. 3(a).

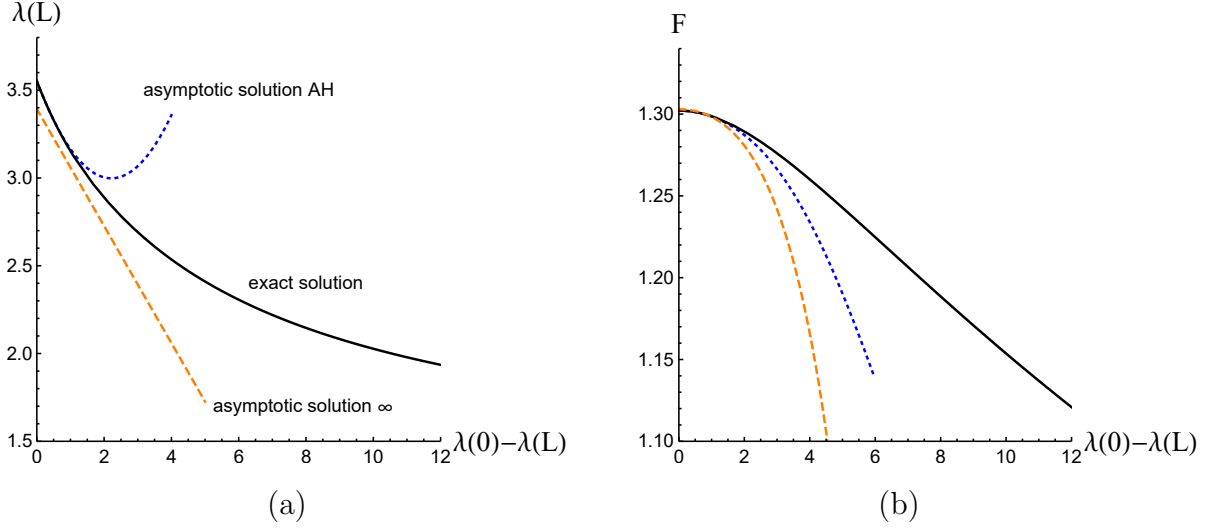


Figure 6: Comparison of two sets of asymptotic results with the exact solution obtained by integrating (4.9) subject to the natural boundary conditions when  $L = 1$ . Solid line (black): exact result; dashed line (orange): current result (4.16); dotted line (blue): asymptotic result of Audoly & Hutchinson (2016).

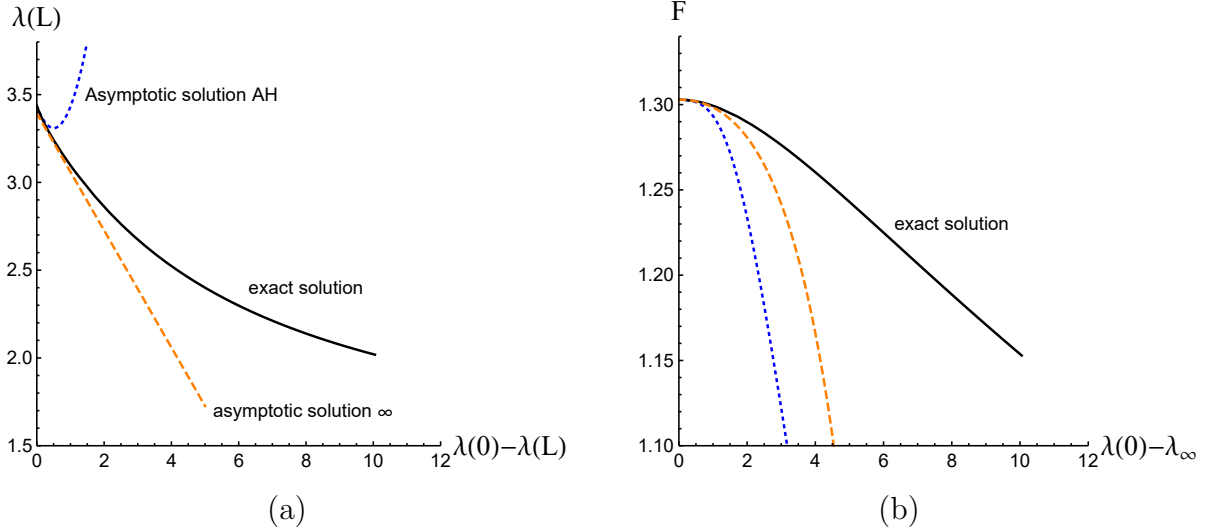


Figure 7: Same as in Fig. 6 except that  $L = 2$ . The results demonstrate the fact that the finite-length cylinder can now effectively be treated as an infinite cylinder.

Secondly, Fig. 6 displays the weakly nonlinear asymptotic result of Audoly & Hutchinson (2016) and our asymptotic result (4.16) together with the exact result for the case  $L = 1$ . The

corresponding results for  $L = 2$  is shown in Fig. 7. In applying (4.16) that is independent of  $L$ , the  $\lambda_\infty$  is identified with  $\lambda(L)$ . It is seen that the results of Audoly & Hutchinson (2016) outperform our results for  $L = 1$  but our results clearly outperform theirs as soon as  $L$  has become as large as 2. Also, although the asymptotic results of Audoly & Hutchinson (2016) have the correct gradient at zero necking amplitude, their rapid curling up and away from the exact solutions in Figs 6(a) and 7(a) are further indications that a weakly nonlinear analysis for localization problems based on a finite critical mode number has a very narrow region of validity.

Finally, we compare the actual profiles of  $r(Z)$  given by the two asymptotic theories. The *two-term* weakly nonlinear results of Audoly & Hutchinson (2016) are obtained by substituting the expansions

$$\lambda = \lambda_{\text{cr}}^* + \varepsilon^2 l_1 + \varepsilon \cos \frac{\pi Z}{L} + \varepsilon^2 d_2 \cos \frac{2\pi Z}{L}, \quad F = n(\lambda_{\text{cr}}^* + \varepsilon^2 l_1) + \varepsilon^2 F_2 \quad (5.7)$$

into (4.9), expanding in terms of  $\varepsilon$ , and then equating the coefficients of like powers of  $\varepsilon$ . The coefficients of  $\varepsilon$ ,  $\varepsilon^2$  and  $\varepsilon^3$  in turn give the bifurcation condition (5.5), expressions for  $d_2$  and  $F_2$ , and expression for  $l_1$ . The small parameter  $\varepsilon$  is determined by the condition that

$$\frac{1}{L} \int_0^L \lambda(Z) dZ = \lambda_{\text{cr}} + \varepsilon^2 l_1, \quad (5.8)$$

where the left hand side is computed with the aid of the exact numerical solution. In applying the *one-term* asymptotic solution (4.12) together with (4.15), the  $\lambda_\infty$  is identified with  $\lambda(L)$  from the exact solution. In Fig. 8, we have shown the two asymptotic solutions together with the exact solution when  $F = 0.999F_{\text{max}}$ . It is seen again that the results of Audoly & Hutchinson (2016) outperform our results for  $L = 1$  but our results outperform theirs when  $L = 2$ . Also note that the two-term asymptotic solution even has the “wrong” shape when  $L = 2$ .

## 6. Conclusion

Localized necking in a stretched plate or cylinder of finite length has previously been studied as a bifurcation from the primary deformation with a non-zero wave number. In other words, necking solutions have previously been approximated by a superposition of periodic functions. Such an approach only applies to certain types of end conditions, and is invalid if, for instance, the ends are fixed. The current paper investigates the validity of the other approach, the one in which the necking problem is treated as a bifurcation with zero wave number. This is in the same spirit as our previous studies on localized bulging of inflated rubber cylinders. When a cylinder of finite length is effectively treated as an infinite cylinder, the question naturally arises as to how long the cylinder should be (when compared

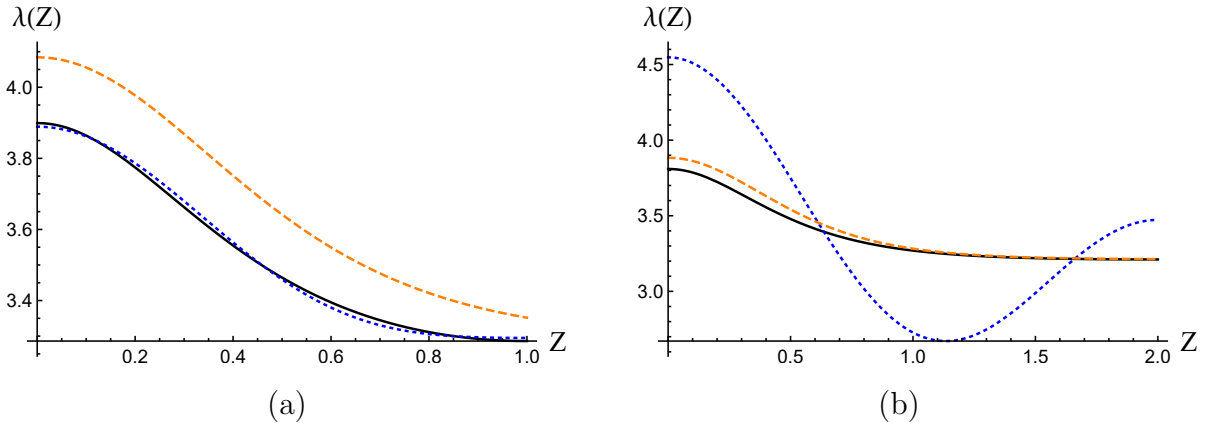


Figure 8: Comparison of the two asymptotic theories with solid (black), dotted (blue), and dashed (orange) lines denoting the exact solution, the two-term asymptotic solution given by (5.7)<sub>1</sub> and the one-term asymptotic solution (4.12) and (4.15) for an infinite cylinder. (a)  $L=1$ ; (b)  $L=2$ .

with the radius) for this approach to be valid. Surprisingly, we find that our approach gives sufficiently accurate results for length/diameter ratios as small as 2 (note, however, that this ratio becomes more than three times larger in the deformed configuration). This is due to the fact that the necking solutions decay exponentially towards the two ends, and furthermore, the further away the load is from the bifurcation value, the more localized the solution. This behaviour can best be described by a homoclinic orbit, whereas any analysis based on a superposition of periodic functions will have limited validity since a large number of sinusoidal terms will be required to approximate a homoclinic solution, especially in the fully nonlinear regime. This approach also has the advantage that it is independent of the end conditions; all types of end conditions are lumped together as imperfections. Our evaluation of the validity of the infinite-length approximation has been made possible by the availability of the 1D model proposed recently by Audoly & Hutchinson (2016). In return, the amplitude equation derived using the exact 3D theory of nonlinear elasticity serves to provide an alternative validation for this powerful 1D model.

#### *Acknowledgements*

This work was supported by the National Natural Science Foundation of China (Grant Nos 11672202).

#### **References**

- Antman, S. S. (1972). Qualitative theory of the ordinary differential equations of nonlinear elasticity. *Mechanics Today* (ed. S. Nemat-Nasser), (pp. 58–101).
- Antman, S. S. (1973). Nonuniqueness of equilibrium states for bars in tension. *J. Math. Anal. Appl.*, 44, 333–349.

- Antman, S. S., & Carbone, E. R. (1977). Shear and necking instability in nonlinear elasticity. *J. Elast.*, *7*, 125–151.
- Audoly, B., & Hutchinson, J. W. (2016). Analysis of necking based on a one-dimensional model. *J. Mech. Phys. Solids*, *97*, 68–91.
- Barenblatt, G. I. (1964). On the neck propagation under tension of polymeric samples. *Appl. Math. Mech.*, *28*, 1048–1060.
- Burke, M. A., & Nix, W. D. (1979). A numerical study of necking in the plane tension test. *Int. J. Solids Struct.*, *15*, 379–393.
- Carothers, W. H., & Hill, J. W. (1932). Studies of polymerization and ring formation xv. artificial fibers from synthetic linear condensation superpolymers. *J. Am. Chem. Soc.*, *54*, 1579–1587.
- Chadwick, P., & Ogden, R. W. (1971). On the definition of elastic moduli. *Arch. Ration. Mech. Anal.*, *44*, 41–53.
- Chen, W. H. (1971). Necking of a bar. *Int. J. Solids Struct.*, *7*, 685–717.
- Coleman, B. D. (1983). Necking and drawing in polymeric fibers under tension. *Arch. Ration. Mech. Anal.*, *83*, 115–137.
- Coleman, B. D., & Newman, D. C. (1988). On the rheology of cold drawing. i. elastic materials. *J. Polymer Sci.*, *26*, 1801–1822.
- Crissman, J. M., & Zapas, I. J. (1974). Creep failure and fracture of polyethylene in uniaxial extension. *Polymer Eng. Sci.*, *19*, 99–103.
- Dai, H.-H., & Bi, Q. S. (2006). On constructing the unique solution for the necking in a hyper-elastic rod. *J. Elast.*, *82*, 215–241.
- Dai, H.-H., Hao, Y. H., & Chen, Z. (2008). On constructing the analytical solutions for localizations in a slender cylinder composed of an incompressible hyperelastic material. *Int. J. Solids Struct.*, *45*, 2613–2628.
- Dai, H.-H., & Peng, X. C. (2012). Elliptic-spline solutions for large localizations in a circular blatz-ko cylinder due to geometric softening. *SIAM J. Appl. Math.*, *72*, 181–200.
- Ericksen, J. L. (1975). Equilibrium of bars. *J. Elast.*, *5*, 191–201.
- Fu, Y. B. (2001). *Nonlinear stability analysis*. In *Nonlinear elasticity: theory and applications* (eds YB Fu, RW Ogden). Cambridge University Press, Cambridge.

- Fu, Y. B., Dorfmann, L., & Xie, Y. X. (2018). Localized necking of a dielectric membrane. *Extreme Mech. Lett.*, *21*, 44–48.
- Fu, Y. B., Jin, L. S., & Goriely, A. (2020). Necking, beading, and bulging in soft elastic cylinders. *J. Mech. Phys. Solids*, *Submitted*.
- Fu, Y. B., & Ogden, R. W. (1999). Nonlinear stability analysis of pre-stressed elastic bodies. *Continuum Mech. Thermodyn.*, *11*, 141–172.
- Fu, Y. B., Pearce, S. P., & Liu, K.-K. (2008). Post-bifurcation analysis of a thin-walled hyperelastic tube under inflation. *Int. J. Non-linear Mech.*, *43*, 697–706.
- Fu, Y. B., & Rogerson, G. A. (1994). A nonlinear analysis of instability of a pre-stressed incompressible elastic plate. *Proc. R. Soc. Lond. A*, *446*, 233–254.
- Hill, R., & Hutchinson, J. W. (1975). Bifurcation phenomena in the plane tension test. *J. Mech. Phys. Solids*, *23*, 239C264.
- Leonov, A. I. (2002). A theory of necking in semi-crystalline polymers. *Int. J. Solids Struct.*, *39*, 5913–5926.
- Mielke, A. (1991). *Hamiltonian and Lagrangian Flows on Center Manifolds, with Applications to Elliptic Variational Problems*. Springer-Verlag (Lecture Notes in Mathematics vol. 1489), Berlin.
- Needleman, A. (1972). A numerical study of necking in circular cylindrical bar. *J. Mech. Phys. Solids*, *20*, 111–127.
- Norris, D. M., Moran, B., Scudder, J. K., & Quinones, D. F. (1978). A computer simulation of the tension test. *J. Mech. Phys. Solids*, *26*, 1–19.
- Ogden, R. W. (1984). *Non-linear Elastic Deformations*. Ellis Horwood, New York.
- Owen, N. (1987). Existence and stability of necking deformations for nonlinearly elastic rods. *Arch. Ratl. Mech. Anal.*, *98*, 357–383.
- Scherzinger, W., & Triantafyllidis, N. (1998). Asymptotic analysis of stability for prismatic solids under axial loads. *J. Mech. Phys. Solids*, *46*, 955–1007.
- Silling, S. A. (1988). Two-dimensional effects in the necking of elastic bars. *J. Appl. Mech.*, *55*, 530–535.
- Triantafyllidis, N., & Aifantis, E. C. (1986). A gradient approach to localization of deformation. i. hyperelastic materials. *J. Elast.*, *16*, 225–237.

- Triantafyllidis, N., Scherzinger, W. M., & Huang, H.-J. (2007). Post-bifurcation equilibria in the plane-strain test of a hyperelastic rectangular block. *Int. J. Solids Struct.*, *44*, 3700–3719.
- Wang, S. B., Guo, G. M., Zhou, L., Li, L. A., & Fu, Y. B. (2019). An experimental study of localized bulging in inflated cylindrical tubes guided by newly emerged analytical results. *J. Mech. Phy. Solids*, *124*, 536–554.
- Ward, I. M., & Sweeney, J. (1982). *Mechanical Properties of Solid Polymers (3rd Ed.)*. Wiley, New York.
- Wesolowski, Z. (1962). Stability in some cases of tension in the light of the theory of finite strain. *Arch. Mech. Stos.*, *14*, 875–900.
- Whitney, W., & Andrews, R. D. (1967). Yielding of glassy polymers: volume effects. *J. Polym. Sci. Part C*, *16*, 2981–2990.
- Wolfram Research Inc. (2019). *Mathematica: version 12.*. Wolfram Research Inc, Champaign, IL.
- Ye, Y., Liu, Y., & Fu, Y. B. (2020). Weakly nonlinear analysis of localized bulging of an inflated hyperelastic tube of arbitrary wall thickness. *J. Mech. Phy. Solids*, *135*, 103804.
- Zapas, I. J., & Crissman, J. M. (1974). An instability leading to failure of polyethylene in uniaxial creep. *Polym. Eng. Sci.*, *19*, 104–107.